

Critical roles of miRNA-mediated regulation of TGF β signalling during mouse cardiogenesis

Yin Peng^{1†}, Lanying Song^{1†‡}, Mei Zhao^{1†¶}, Cristina Harmelink^{1§}, Paige Debenedittis^{1§}, Xiangqin Cui², Qin Wang³, and Kai Jiao^{1*}

¹Division of Research, Department of Genetics, The University of Alabama at Birmingham, 720 20th St. S., 768 Kaul Building, Birmingham AL 35294, USA; ²Department of Biostatistics, The University of Alabama at Birmingham, Birmingham, USA; and ³Department of Cell, Developmental and Integrative Biology, The University of Alabama at Birmingham, Birmingham, USA

Received 2 July 2013; revised 9 April 2014; accepted 1 May 2014; online publish-ahead-of-print 16 May 2014

Time for primary review: 33 days

Aims	MicroRNAs (miRNAs) play critical roles during the development of the cardiovascular system. Blocking miRNA biosynthesis in embryonic hearts through a conditional gene inactivation approach led to differential cardiac defects depending on the Cre drivers used in different studies. The goal of this study is to reveal the cardiogenic pathway that is regulated by the miRNA mechanism at midgestation, a stage that has not been evaluated in previous publications.
Methods and results	We specifically inactivated <i>Dicer1</i> , which is essential for generation of functional mature miRNAs, in the myocardium by crossing <i>cTnt-Cre</i> mice with <i>Dicer1</i> ^{loxP} mice. <i>cTnt-Cre</i> efficiently inactivates target genes in cardiomyocytes at midgestation. All mutants died between E14.5 and E16.5 with severe myocardial wall defects, including reduced cell proliferation, increased cell death, and spongy myocardial wall. Expression of TGF β type I receptor (<i>Tgfb1</i>), which encodes the Type I receptor of TGF β ligands, was up-regulated in mutant hearts. As expected, TGF β activity was increased in <i>Dicer1</i> -inactivated hearts. Our further molecular analysis suggested that <i>Tgfb1</i> is a direct target of three miRNAs. Reducing TGF β activities using a pharmacological inhibitor on <i>in vitro</i> cultured hearts, or through an <i>in vivo</i> genetic approach, partially rescued the cardiac defects caused by <i>Dicer1</i> inactivation.
Conclusions	We show for the first time that TGF β signalling is directly regulated by the miRNA mechanism during myocardial wall morphogenesis. Increased TGF β activity plays a major role in the cardiac defects caused by myocardial deletion of <i>Dicer1</i> . Thus, miRNA-mediated regulation of TGF β signalling is indispensable for normal cardiogenesis.
Keywords	TGF β • MicroRNAs • Cardiogenesis

1. Introduction

TGF β signalling is critical for cardiovascular development; abnormal TGF β activities cause various congenital cardiovascular defects in both animal models and human patients.^{1–5} The intracellular signalling cascade activated by TGF β cytokines (including TGF β 1, TGF β 2, and TGF β 3) has extensively been studied. In brief, a TGF β ligand homodimer binds and brings together the Type I and II serine/threonine kinase receptors at the cell membrane to form the ligand–receptor complex, which allows the Type II receptor to phosphorylate the

Type I receptor. The activated Type I receptor subsequently phosphorylates the cytoplasmic proteins SMAD2 and SMAD3. Phosphorylated SMAD2 and SMAD3 (p-SMAD2 and p-SMAD3) associate with SMAD4 and translocate to the nucleus to regulate transcription of target genes.^{6,7} In addition to the SMAD pathway, TGF β signalling can also activate non-canonical kinase pathways.^{8–10}

TGF β signalling plays critical roles during cardiogenesis. *Tgfb2*^{-/-} mice display a range of congenital heart defects (CHDs), including double outlet right ventricle, septal defects, and an overriding tricuspid valve.^{11,12} Endothelial inactivation of genes encoding the TGF β type I

* Corresponding author. Tel: +1 205 996 4198; fax: +1 205 975 5689, Email: kjiao@uab.edu

† Y.P., L.S. and M.Z. contributed equally to the work.

‡ Present address. Department of Molecular Biosciences, University of California, Davis, CA, USA.

¶ Present address. Department of Cardiology, Shengjing Hospital, China Medical University, China.

§ Present address. Department of Pediatric Cardiology, Vanderbilt University Medical Center, Nashville, TN, USA.

(*Tgfb1*) or the type II (*Tgfb2*) receptors has led to severe valvuloseptal defects.^{13,14} Intriguingly, cardiomyocyte inactivation of *Tgfb1* or *Tgfb2* did not cause obvious cardiac defects in the majority of embryos.^{13,14} The activities of the two genes in the myocardium are likely compensated by other genes encoding TGF β superfamily receptors. Even though *Tgfb1* and *Tgfb2* are not essential for myocardial development, these results do not exclude the possibility that up-regulation of these two genes in cardiomyocytes may cause heart defects. Supporting this idea, in a transgenic study, constitutively activated myocardial TGFBR1 led to the arrest of heart development at the looping stage and resulted in ventricular hypoplasia.¹⁵

Human genetic studies provide direct evidence supporting the clinical significance of altered TGF β signalling in the aetiology of inborn cardiovascular anomalies. *TGFBR1* and *TGFBR2* are causal genes for Marfan syndrome and Loeys–Dietz syndrome,^{16–19} both of which are associated with CHDs. Also, mutations in *TGFBR2* and *SMAD3* cause syndromic aortic aneurysms.^{20–22} Significantly, mutations in these genes may either decrease or increase TGF β signalling in patients,^{16–19} indicating that maintaining the proper level of TGF β activity is critical for cardiovascular development.

The microRNA (miRNA) machinery plays vital roles during cardiogenesis.^{23–25} miRNAs are evolutionarily conserved non-coding small RNA molecules that primarily act on the 3' untranslated regions (UTRs) of target mRNAs to down-regulate their stability and translation efficiency.^{23–25} Genes encoding miRNAs are transcribed by RNA polymerase II/III to generate Pri-miRNAs, which are processed to Pre-miRNAs by DROSHA in the nucleus. Pre-miRNAs are exported to the cytoplasm, where they are further processed by the RNase III ribonuclease DICER to generate ~22 nucleotide mature miRNAs. Therefore, DICER is required for the generation of most, if not all, functional miRNAs. In metazoans, the 'seed' sequence, referring to nucleotides 2–8 of a miRNA, is typically 100% complementary to its target.²⁶

To understand the cardiogenic roles of global miRNA biosynthesis, *Dicer1* has been inactivated in cardiomyocytes at precursor and late gestational stages.^{27–29} These studies collectively indicate that miRNAs play complex roles at different stages. In our current study, we specifically inactivated *Dicer1* in the myocardium during midgestation, a stage that has not been evaluated in published studies. We revealed that TGF β signalling is directly regulated by the miRNA machinery in developing hearts, and that such regulation is indispensable for normal myocardial wall development.

2. Methods

2.1 Mouse maintenance, genotyping, and tissue processing

This study conforms to the Guide for the Care and Use of Laboratory Animals published by the US National Institutes of Health (NIH Publication no. 85-23, revised 1996). All protocols were approved by the Institutional Animal Care and Use Committee at the University of Alabama at Birmingham. Euthanasia of mice was achieved through inhalation of CO₂. Generation of the *cTnt-Cre*,³⁰ *Dicer1*^{loxP/loxP},³¹ and *Tgfb2*^{loxP/loxP}³² lines has been described previously. Mice are on a mixed C57Bl/6 \times 129s6 background. Primers and polymerase chain reaction (PCR) conditions for genotyping were described previously.^{30–32}

2.2 Cell culture, transfection, generation of reporter constructs, and luciferase assay

COS-M6 cells³³ and the NkL-TAG cardiomyocyte cells³⁴ were cultured as previously described. Lipofectamine2000 and Neon Electroporation

System (Invitrogen) were used for transfection. miRNA mimics were purchased from Ambion. To generate reporter constructs, a ~400 bp fragment within the 3' UTR of *mTgfb1* containing a potential miRNA target site was cloned into the pMIR-REPORT-LUC vector (Ambion). Luciferase activities were measured using the Luciferase assay kit (Promega). A plasmid expressing a lacZ reporter driven by a constant promoter was co-transfected for normalization of transfection efficiency. LacZ activity was measured using the Beta-Glo-Assay System (Promega).

2.3 Microarray and quantitative reverse transcription-PCR analysis

Total RNA isolated with the RNeasy Plus Kit (Qiagen) from E13.5 hearts was subjected to microarray analysis using the Affymetrix GeneChip Mouse Genome 430 2.0 Array (UAB Heflin Genomic Core). Data were averaged from two independent experiments. Reverse transcription was performed using SuperScriptIII (Invitrogen). Quantitative PCR analysis was performed using LightCycler480 SYBR Green I Master (Roche) on the Roche LightCycler480 Real-Time PCR machine. *Hprt* was used as a loading control. The primers for RT-PCR are listed in Supplementary material online. miRNA was isolated using the mirVana miRNA Isolation Kit (Ambion) followed by quantitative reverse transcription (qRT)-PCR using the TaqMan miRNA RT Kit and TaqMan Universal PCR Master Mix (Ambion).

2.4 Purification of cardiomyocytes using a molecular Beacon

Embryonic hearts at E11.5–12.0 were digested with 0.05% trypsin for 10–20 min to acquire single-cell suspension. Cells were spin down and re-suspended in PBS. The molecular beacon, MHC1-MB,³⁵ was transfected into cells using the Neon Electroporation Transfection System. DMEM with 10% fetal bovine serum (FBS) was then added to cells. After 0.5-h recovery in a 37°C cell culture incubator, cells were sorted using the FACSAria sorter in the UAB Flow Cytometry Facility core. Right after purification of cells, RNA was isolated and RT-PCR using primers for myocardial- and endocardial-specific genes was performed to confirm the purity of isolated cardiomyocytes. qRT-PCR using primers corresponding to the floxed region of *Dicer1* cDNA was performed to test if expression of *Dicer1* mRNA was reduced in mutants. The MHC1-MB beacon with 5' 6-FAM and 3' BlackHole-Quencher I can efficiently label cardiomyocytes with a high specificity³⁵ and was synthesized from integrated DNA technologies.

2.5 Western, immunostaining, and *in situ* hybridization analysis

Total protein was isolated and quantified using DC Protein Assay Kit (Biorad). For western analysis, equal amounts of protein were separated through SDS-PAGE, and transferred to the PVDF membrane (Biorad). The filter was incubated with primary antibody overnight at 4°C. On the second day, the filter was washed and incubated with a horseradish peroxidase-conjugated secondary antibody (Invitrogen) for 1 h. Signals were visualized using the ECL kit (Millipore). Embryos were dissected in PBS and fixed in 4% paraformaldehyde overnight. The next day, tissues were dehydrated, cleared with Histo-Clear, and embedded in wax. Wax blocks were sectioned at 8–10 μ m. For immunofluorescence studies, embryonic sections were dewaxed, re-hydrated, treated with 10 mM sodium citrate (pH 6.0) for antigen retrieval, and incubated with primary antibodies overnight at 4°C. The next day, Alexa Fluor-conjugated secondary antibodies (Invitrogen) were used to visualize the signal. Samples were counterstained with DAPI to visualize total nuclei. The primary antibodies include cleaved Caspase3 (#9661), p-SMAD2 (#3101), total SMAD2 (#3102), p-SMAD3 (#9520) (Cell Signaling), Actc1 (AC1-20.4.2), Actinin (EA53) (Sigma), ACVR1B (ab64813), MLC1v (MLM527), cTnC (3A10A12), SMAD7 (ab76498) (Abcam), cTnt (CT3), MHC (MF20), Tropomyosin (CH1), Tubulin (E7), Vimentin (40E-C) (Iowa Hybridoma Bank), DICER1 (sc30226), GAPDH (A3), MLC2v (sc3449), TGFBR1(sc398) (Santa Cruz),

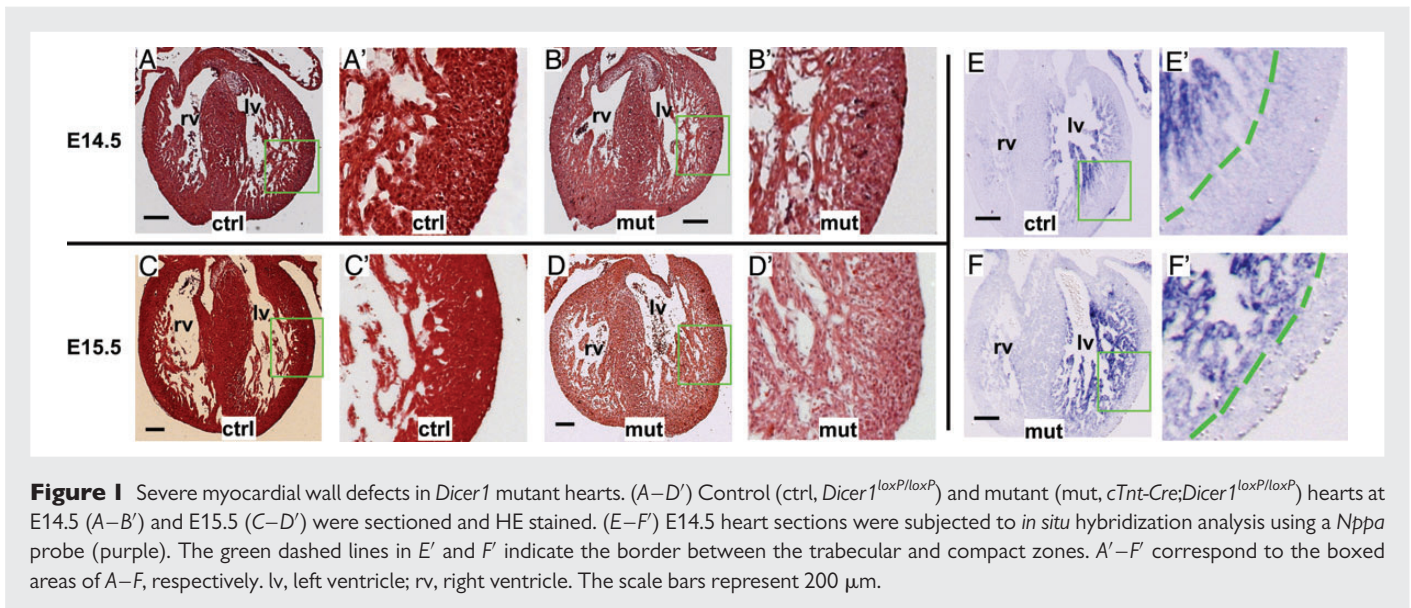


Figure 1 Severe myocardial wall defects in *Dicer1* mutant hearts. (A–D') Control (ctrl, *Dicer1*^{loxP/loxP}) and mutant (mut, *cTnt-Cre*;*Dicer1*^{loxP/loxP}) hearts at E14.5 (A–B') and E15.5 (C–D') were sectioned and HE stained. (E–F') E14.5 heart sections were subjected to *in situ* hybridization analysis using a *Nppa* probe (purple). The green dashed lines in E' and F' indicate the border between the trabecular and compact zones. A'–F' correspond to the boxed areas of A–F, respectively. lv, left ventricle; rv, right ventricle. The scale bars represent 200 μ m.

phospho-Histone H3 (pH3, 06-570) (Millipore), and total SMAD3 (ThermoScientific). The anti-MLC2a antibody was provided by S. Kubalak (University of South Carolina). Section *in situ* hybridization analysis was performed as previously described.³⁶

2.6 Deoxynucleotidyl transferase dUTP nick end labelling and EdU labelling experiments

Transferase dUTP nick end labelling (TUNEL) assays were performed using the DeadEnd Fluorescence TUNEL system (Promega). For EdU labelling experiments, E14.5 hearts were cultured in DMEM containing 10% FBS and 10 μ M EdU (Invitrogen) for 2 h at 37°C. Samples were then embedded in wax and sectioned. EdU signals were detected using the Click-iT-EdU Imaging Kit (Invitrogen).

3. Results

3.1 Inactivation of *Dicer1* at midgestation leads to severe myocardial wall defects

To better understand the roles of miRNA-mediated gene regulation during cardiogenesis, we crossed male *cTnt-Cre*;*Dicer1*^{loxP/+} mice with female *Dicer1*^{loxP/loxP} mice to acquire mutant animals (*cTnt-Cre*;*Dicer1*^{loxP/loxP}). *cTnt-Cre* efficiently inactivates target genes in the myocardium during midgestation.^{30,37} The *Dicer1* mRNA in purified cardiomyocytes from mutant hearts (E11.5–12.0) was reduced to <1% of the control level (see Supplementary material online, Figure S1A and B). Western analysis confirmed reduced expression of DICER1 (see Supplementary material online, Figure S1C). The level of mature miR1 was significantly reduced in mutants (see Supplementary material online, Figure S1D). miR1 is highly expressed in the myocardium and its maturation relies on *Dicer1*.²⁹ Our data collectively indicated that *Dicer1* was efficiently inactivated in mutant cardiomyocytes at midgestation.

No mutants were identified from newborn pups, indicating lethality of mutant embryos. The ratio of living mutant embryos was close to the expected 25% through E14.5 (see Supplementary material online, Figure S2). At E15.5, the ratio of living mutants dropped to ~15% and no living mutants could be identified beyond E16.5. Our histological examination did not reveal apparent defects in mutants until E13.5. At E14.5, the myocardial walls of mutants appeared to be spongier than

those of controls (Figure 1A and B'), suggesting defects in myocardial wall compaction. The spongy ventricles in mutants became more dramatic at E15.5 (Figure 1C and D'). No defect was observed in valves of mutant hearts. *In situ* hybridization analysis using a *Nppa* probe, which specifically stains the trabecular region of left ventricles,³⁸ confirmed that the trabecular zone was increased and the compaction zone was decreased in mutant hearts (Figure 1E and F'). Similar results were acquired from *in situ* hybridization analysis using a *Bmp10* probe (see Supplementary material online, Figure S3). Expression of *cTnt* was reduced, but not eliminated in some areas in the compact zone of mutant ventricles (see Supplementary material online, Figure S4).

3.2 Mutant hearts display abnormal cell proliferation, apoptosis, and expression of contractile proteins

To reveal the cellular defects caused by myocardial inactivation of *Dicer1*, we performed immunostaining studies using an anti-pH3 antibody and found significantly reduced cell proliferation in mutant hearts at E13.5 (Figure 2A–C). Our TUNEL analysis revealed significantly increased apoptosis in mutants (Figure 2D–F). Expression of a group of contractile proteins, such as Actinin, cTnC, MHC, MLC1V, and MLC2V, was reduced in mutants (Figure 2G), whereas expression of ACTC1, MLC2A, and Tropomyosin was not altered (see Supplementary material online, Figure S5). Misexpression of contractile proteins was also reported in mice with *Dicer1* inactivation at a later stage.²⁹

3.3 Expression of TGFBR1 is up-regulated in mutant hearts

To identify genes whose expression is regulated by *Dicer1*, we performed microarray analysis on control and mutant hearts at E13.5. Since miRNAs negatively regulate gene expression, we focused on the up-regulated genes in mutant hearts. A total of 17 genes were identified as up-regulated by at least 1.5-fold in mutants (see Supplementary material online, Table S1). Significantly, the expression of *Tgfb1* was increased by 1.9-fold, suggesting the involvement of miRNAs in regulating TGF β signalling. We confirmed that the level of *Tgfb1* mRNA was increased by qRT-PCR (Figure 3A) and *in situ* hybridization analysis

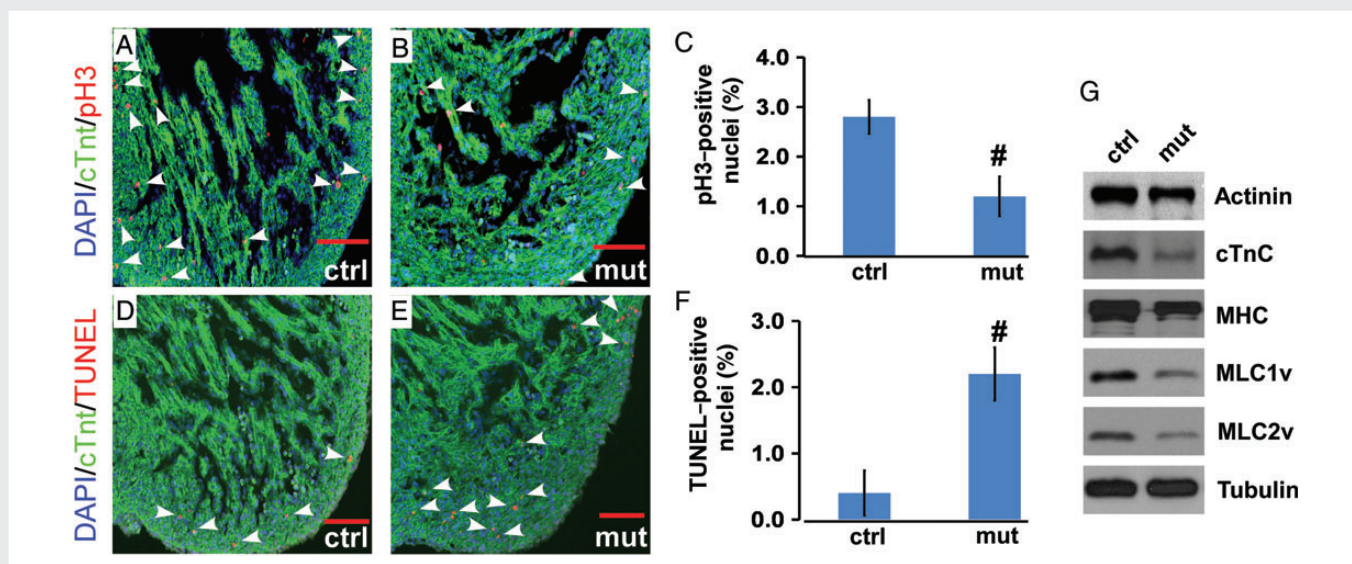


Figure 2 Cellular defects caused by myocardial inactivation of *Dicer1*. (A–C) Control (ctrl, *Dicer1*^{loxP/loxP}) and mutant (mut, *cTnt-Cre*;*Dicer1*^{loxP/loxP}) hearts (E13.5) were immunostained with an anti-pH3 antibody (red) and an anti-cTnt antibody (green). Total nuclei were visualized with DAPI (blue). (D–F) E13.5 heart sections were subjected to the TUNEL assay (red), followed by immunostaining with a cTnt antibody (green). Data in C and F were averaged from at least four embryonic hearts of each genotype. For each heart, at least two sections were counted. For each section, we counted a total of 600 cTnt-positive cells (200 cells for each structure of the ventricular septum, right ventricle, and left ventricle). Error bars indicate standard deviation (SD). #*P* < 0.01 (Student's *t*-test). (G) Protein lysates from E13.5 hearts were subjected to western analysis using antibodies as indicated. Tubulin was used as the loading control. Arrow heads indicate examples of positively stained cells. Scale bars represent 50 μ m.

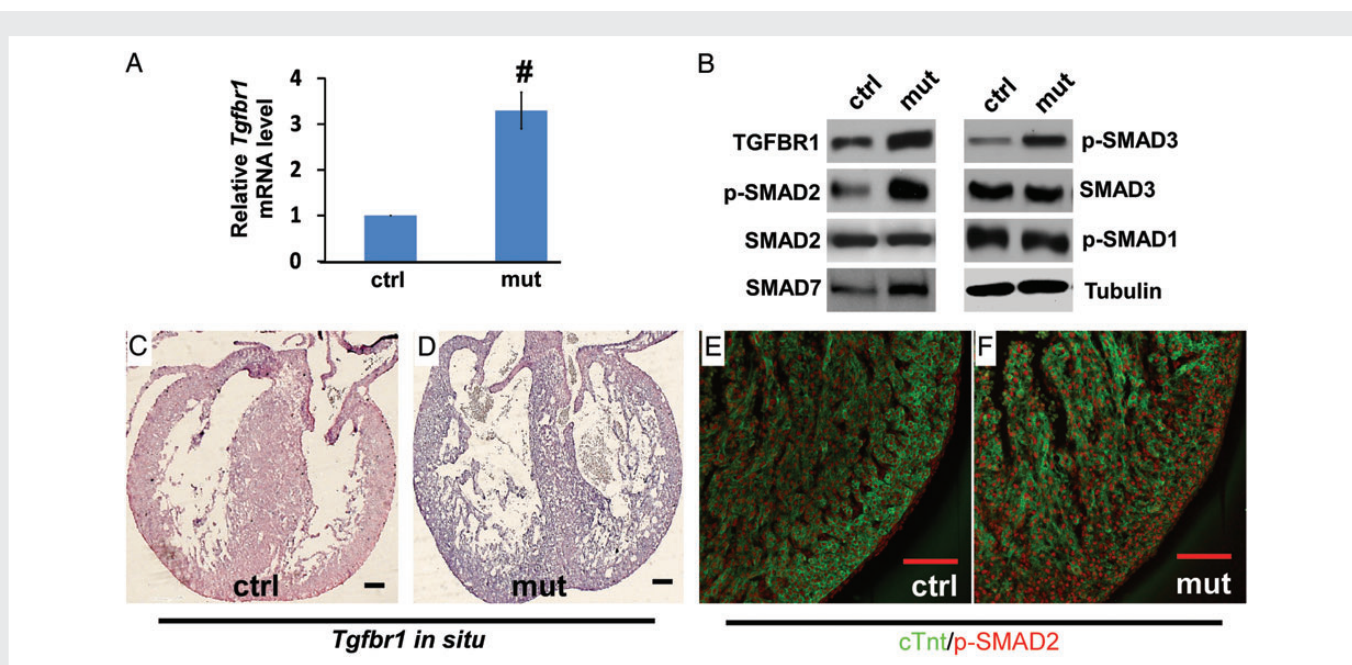


Figure 3 Up-regulated TGF β signalling in mutant hearts. (A) qRT-PCR analysis of *Tgfbf1* using total RNA isolated from control (ctrl, *Dicer1*^{loxP/loxP}) and mutant (mut, *cTnt-Cre*;*Dicer1*^{loxP/loxP}) hearts at E13.5. Error bars indicate SD. #*P* < 0.01 (Student's *t*-test, *n* \geq 4). (B) Protein lysates isolated from E13.5 hearts were subjected to western analysis using various antibodies. (C and D) E13.5 heart sections were subjected to *in situ* hybridization analysis using a *Tgfbf1* probe (purple) and were counterstained with eosin (red). (E and F) Heart sections (E13.5) were immunostained with an anti-p-SMAD2 antibody (red) and a cTnt antibody (green). Identical experimental conditions were applied to control and mutant samples. Scale bars represent 50 μ m.

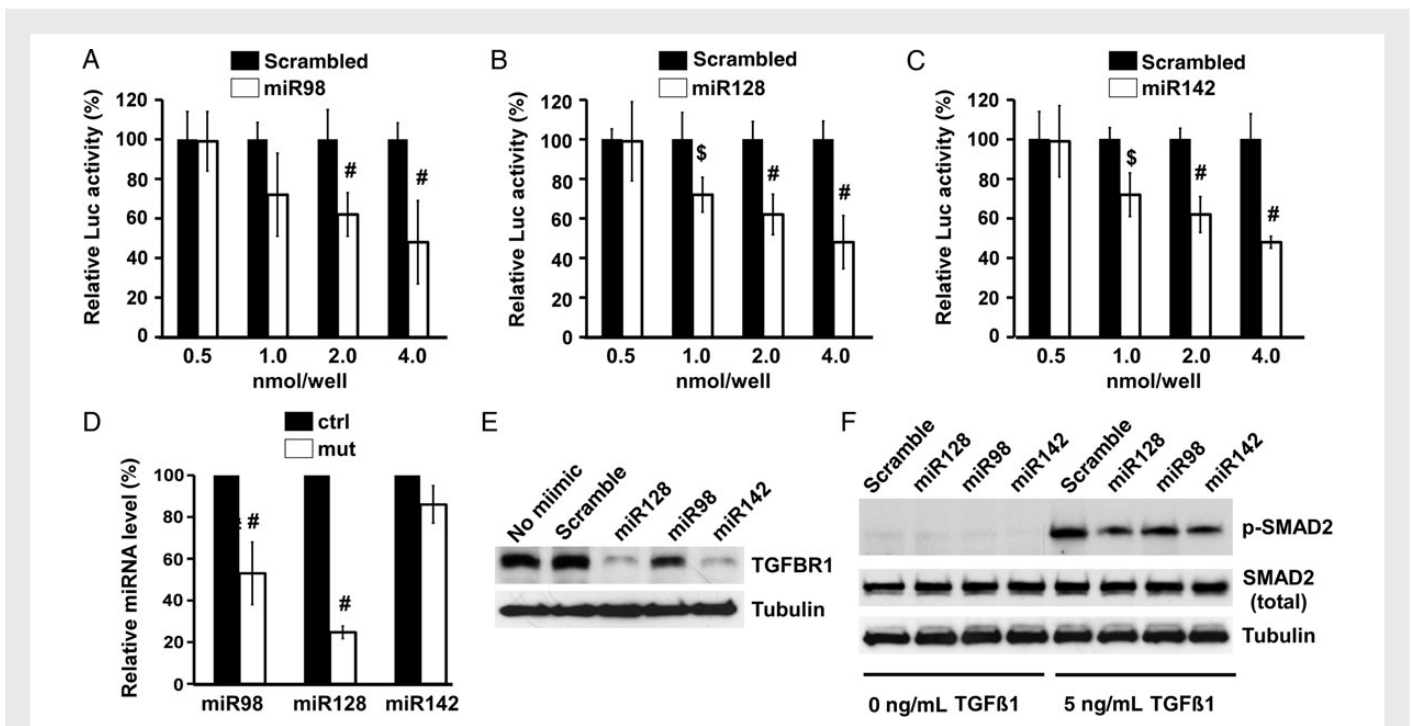


Figure 4 The 3' UTR of *Tgfb1* is targeted by multiple miRNAs. (A–C) Reporter constructs for miR98 (A), miR128 (B), and miR142 (C) were co-transfected into COS-M6 cells with a scrambled control or a corresponding miRNA mimic. The amount of scrambled control or miRNA mimics used in each well of a 24-well plate was as indicated. The luciferase activity of cells containing the scrambled control was set at 100%. Data were averaged from at least three experiments with error bars indicating SD. (D) miRNAs were extracted from control (ctrl, *Dicer1*^{loxP/loxP}) and mutant (mut, *cTnt-Cre;Dicer1*^{loxP/loxP}) hearts at E13.5 and were subjected to qRT-PCR analysis to detect mature miR98, miR128, and miR142. SnoRNA202 was used as a loading control. The level of signal in control hearts was set at 100%. Data were averaged from at least three independent experiments. (E) NkL-TAg cells were transfected with a scrambled control or various miRNA mimics. At 48 h after transfection, western analysis was performed to detect the expression of TGFBR1. The reduction of TGFBR1 by the miR98 mimic was moderate, and yet could be repeatedly detected from four independent experiments. (F) NkL-TAg cells harbouring the scrambled control or various miRNA mimics were treated with 0 or 5 ng/mL of TGFβ1 (R&D) for 4 h, followed by western analysis using antibodies against p-SMAD2, total SMAD2, or tubulin. Reduction of p-SMAD2 was moderate in cells harbouring miR98 and yet could be repeatedly detected. \$*P* < 0.05; #*P* < 0.01 (Student's *t*-test).

(Figure 3C and D). Increased expression of the TGFBR1 protein was confirmed with western analysis (Figure 3B). We next compared the level of p-SMAD2 and p-SMAD3 (active form of TGFβ R-SMADs) between control and mutant hearts (Figure 3E and F), and confirmed the increased TGFβ activity in mutant hearts. Expression of SMAD7, which is a direct downstream target of TGFβ R-SMADs,^{39,40} was also increased in mutant hearts. The level of active SMAD1 (p-SMAD1) was not altered by inactivation of *Dicer1*, indicating that bone morphogenetic protein activity was not affected.

3.4 *Tgfb1* mRNA is regulated by multiple miRNAs

Sequence analysis using the TargetScan miRNA target prediction programme (http://www.targetscan.org/mmu_61/) identified three potential miRNA target sites within the 3' UTR of *Tgfb1* that are conserved among vertebrates, including humans (see Supplementary material online, Figure S6). These sites are 100% matched with the 8 bp seed sequences of miR98/let7, miR128, and miR142, respectively. The three putative sites were confirmed using two additional independent miRNA target prediction programmes, including miRWalk (<http://www.umm.uni-heidelberg.de/apps/zmf/mirwalk/predictedmirnagene.html>) and MiRanda (<http://www.ebi.ac.uk/enright-srv/microcosm/htdocs/targets/v5/>). To test whether the 3' UTR of *Tgfb1* mRNA is targeted

by the three miRNAs, we generated reporter constructs for each miRNA. The reporter activity for each construct decreased in a dose-dependent fashion when co-transfected with its corresponding miRNA mimic (Figure 4A–C). A scrambled miRNA mimic did not alter the activity of these reporters (see Supplementary material online, Figure S7). We next showed that mature miR98 and miR128 were significantly decreased in mutants (*P* < 0.05, Student's *t*-test) (Figure 4D). The reduction of mature miR142 in mutants was moderate (*P* = 0.07). Thus, miR142 is likely a long-lived miRNA. These results suggest that reduced mature miR98 and miR128 contribute to the increased expression of *Tgfb1* in mutant hearts. Finally, we showed that the three miRNAs can regulate endogenous TGFβ activity. After transfection into NkL-TAg cardiomyocytes,³⁴ all three mimics reduced expression of TGFBR1 (Figure 4E), activation of SMAD2 upon TGFβ stimulation (Figure 4F and see Supplementary material online, Figure S8A), and activity of the SBE4-Lux TGFβ reporter⁴¹ (see Supplementary material online, Figure S8B).

3.5 Blocking TGFBR1 activity alleviates the cardiomyocyte apoptosis defect in mutant hearts *in vitro*

We tested whether increased TGFβ activity has any detrimental effect on embryonic hearts at midgestation. Treatment of *in vitro* cultured

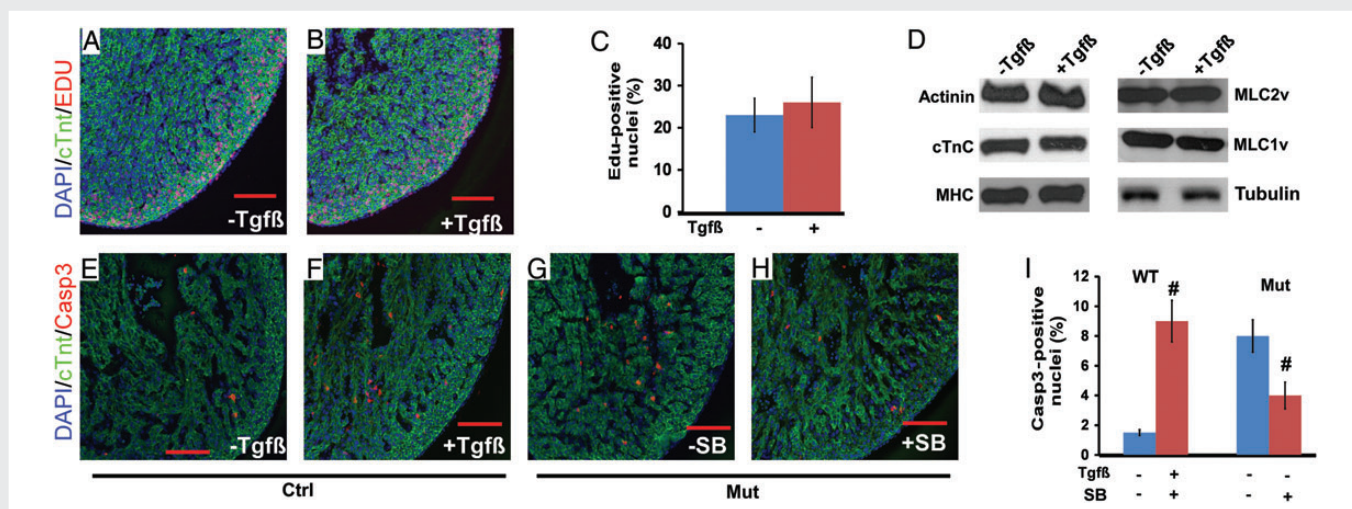


Figure 5 The effect of TGFβ treatment on cultured embryonic hearts. (A–C) *Dicer1*^{loxP/loxP} hearts at E13.5 were isolated, cultured in DMEM with 10% FBS, treated with 5 ng/mL of TGFβ1, and labelled with EdU for 2 h in a 37°C cell culture incubator. EdU-positive nuclei were red. Sections were then subjected to immunostaining with a cTnT antibody (green) and DAPI staining (blue). (C) The quantitative results averaged from three independent hearts. Error bars represent SD. (D) Control hearts at E13.5 were treated with 5 ng/mL of TGFβ1 for 24 h followed by western analysis using primary antibodies as indicated. (E–I) Control (ctrl, *Dicer1*^{loxP/loxP}) embryonic hearts (E and F) were treated with 5 ng/mL of TGFβ1 for 2 h. Embryonic hearts were sectioned and immunostained with an anti-cleaved Caspase 3 antibody (red) and a cTnT antibody (green). Mutant (mut, *cTnT-Cre;Dicer1*^{loxP/loxP}) hearts (G and H) at E13.5 were treated with SB505124. After a 2-h treatment, embryonic hearts were sectioned and immunostained with an anti-cleaved Caspase 3 antibody (red) and a cTnT antibody (green). Data were averaged from at least three independent experiments with error bars showing SD. (I) #*P* < 0.01 (Student's *t*-test). Scale bars represent 50 μm.

Table 1 Genotype distribution of survival embryos between E16.5 and E18.5^a

Genotypes	# of survived embryos
<i>cTnT-Cre;Dicer1</i> ^{loxP/+} ; <i>Tgfr2</i> ^{loxP/+}	28 (24) ^b
<i>cTnT-Cre;Dicer1</i> ^{loxP/+} ; <i>Tgfr2</i> ^{loxP/loxP} ^c	32 (24)
<i>cTnT-Cre;Dicer1</i> ^{loxP/loxP} ; <i>Tgfr2</i> ^{loxP/+} ^d	0 (24)
<i>cTnT-Cre;Dicer1</i> ^{loxP/loxP} ; <i>Tgfr2</i> ^{loxP/loxP} ^e	5 (24)
<i>Dicer1</i> ^{loxP/+} ; <i>Tgfr2</i> ^{loxP/+}	34 (24)
<i>Dicer1</i> ^{loxP/+} ; <i>Tgfr2</i> ^{loxP/loxP}	31 (24)
<i>Dicer1</i> ^{loxP/loxP} ; <i>Tgfr2</i> ^{loxP/+}	28 (24)
<i>Dicer1</i> ^{loxP/loxP} ; <i>Tgfr2</i> ^{loxP/loxP}	33 (24)

^aMale *cTnT-Cre;Dicer1*^{loxP/+}; *Tgfr2*^{loxP/+} mice were crossed with *Dicer1*^{loxP/loxP}; *Tgfr2*^{loxP/loxP} female mice. Embryos between E16.5 and E18.5 were dissected and genotyped.

^bThe number in the parenthesis refers to the expected number from Mendelian ratio.

^c*Tgfr2* sKO embryos.

^d*Dicer1*-sKO embryos.

^e*Dicer1; Tgfr2* dKO embryos.

E14.5 hearts with TGFβ1 did not alter cell proliferation or expression of contractile proteins (Figure 5A–D). Therefore, the enhanced TGFβ activity does not likely contribute to abnormal cell proliferation or expression of contractile proteins as observed in *Dicer1*-inactivated hearts. On the contrary, TGFβ treatment significantly increased cell death in cultured hearts (Figure 5E and F) (*P* < 0.01, Student's *t*-test). Blocking TGFβR1 activity with SB505124⁴² significantly alleviated the apoptosis defect in *Dicer1* mutant hearts (Figure 5G–I). Apoptosis in mutants treated with SB505124 was still higher than the control level, indicating that TGFβR1 blockade partially rescues the cell death defect caused by myocardial inactivation of *Dicer1*.

3.6 Reducing TGFβ activity partially rescues the heart defects caused by inactivation of *Dicer1* in vivo

We applied a genetic approach to determine whether reducing TGFβ activity could alleviate the heart defects caused by *Dicer1* inactivation in vivo. TGFβ activity was reduced through breeding strategies using *Tgfr2*^{loxP/loxP} mice.¹³ TGFβR2 is the only known Type II receptor for TGFβ ligands^{6,7} and activates TGFβR1 upon TGFβ stimulation. We crossed *cTnT-Cre;Dicer1*^{loxP/+}; *Tgfr2*^{loxP/+} mice with *Dicer1*^{loxP/loxP}; *Tgfr2*^{loxP/loxP} mice. Among 191 embryos from 34 litters that survived to E16.5–E18.5, we obtained five double-knockout embryos (dKO, *cTnT-Cre;Dicer1*^{loxP/loxP}; *Tgfr2*^{loxP/loxP}, expecting 24 embryos), and 0 *Dicer1*-single-knockout embryo (sKO, *cTnT-Cre;Dicer1*^{loxP/loxP}; *Tgfr2*^{loxP/+}, expecting 24 embryos). The ratio of embryos with different genotypes is listed in Table 1. The ratio of survival of dKO embryos (2.6%) is significantly lower than the expected Mendelian ratio (12.5%) and significantly higher than that of *Dicer1*-sKO embryos (0%) (*P* < 0.01, χ^2 test). Figure 6 shows an example of a living dKO embryo at E16.5. The ventricular wall of dKO hearts was thinner than controls, but did not show the spongy phenotype (Figure 6A'' and B''). We did not observe any myocardial wall defect in *Tgfr2* sKO embryos. Our western analysis showed that the level of p-SMAD2 was slightly reduced in *Tgfr2* sKO embryonic hearts (see Supplementary material online, Figure S9). The level of p-SMAD2 in dKO embryonic hearts dropped to about the same level observed in *Tgfr2* sKO hearts, confirming the reduced TGFβ activity in dKO hearts. We conclude that reducing TGFβ activity can partially rescue the heart defects caused by myocardial inactivation of *Dicer1* in vivo. In the developing yolk sac, expression of *Actr1b* (*Alk4*) is up-regulated in compensation for the inactivation of TGFβ signalling.⁴³ We therefore examined the expression of ACTR1B. As shown in Supplementary material online, Figure S9, expression of ACTR1B was slightly increased in

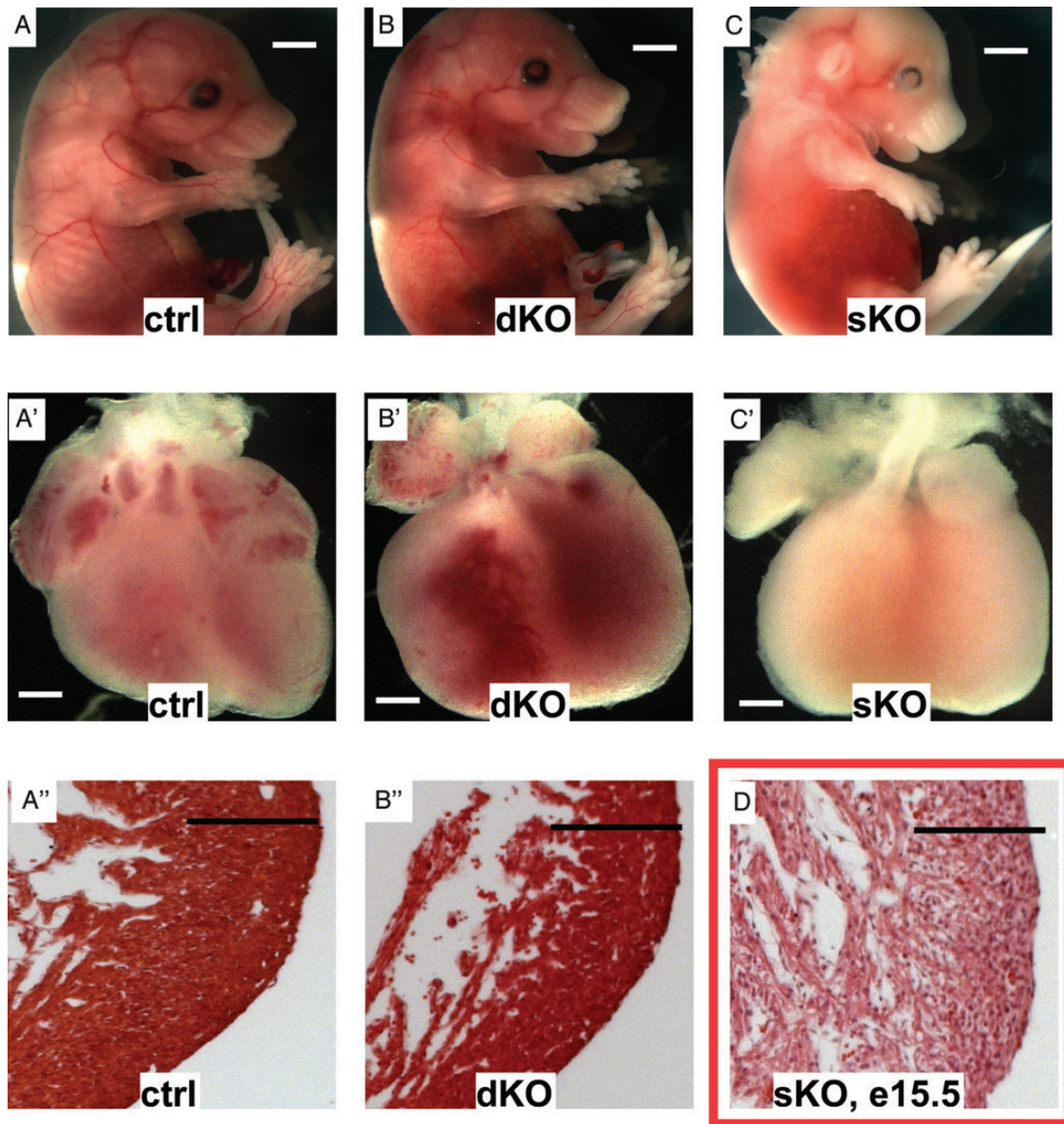


Figure 6 Inactivation of *Tgfb2* partially rescued the heart defects caused by *Dicer1* inactivation. (A–C) Control (ctrl, *Dicer1*^{loxP/loxP}; *Tgfb2*^{loxP/loxP}), dKO (*cTnt-Cre*; *Dicer1*^{loxP/loxP}; *Tgfb2*^{loxP/loxP}), and sKO (*cTnt-Cre*; *Dicer1*^{loxP/loxP}; *Tgfb2*^{loxP/+}) embryos at E16.5 were obtained from the same litter. The ctrl and dKO embryos were alive; while the sKO embryo was dead. (A'–C') Embryonic hearts were isolated from embryos A–C. (A'' and B'') Frontal sections of a control (A'') and a dKO (B'') hearts at E16.5 were HE stained. Left ventricular walls are shown. (D) No sKO mouse survived to E16.5. A sKO heart at E15.5 was shown for comparison. Panel D is identical to D' of Figure 1. Scale bars in (A–C) represent 200 μ m and in (A'–D) represent 50 μ m.

Tgfb2 inactivation and dKO hearts, suggesting that Activin signalling is enhanced by inactivation of *Tgfb2*. We speculate that, in the absence of *Tgfb2*, SMAD2 is phosphorylated by Activin signalling in embryonic hearts.

We also examined cell proliferation/apoptosis in sKO and dKO hearts (see Supplementary material online, Figure S10). A small group (25%) of dKO hearts showed reduced cell death; the apoptosis rate of these embryos is close to the control level, lower than that of sKO or the majority of dKO embryonic hearts. Our results therefore suggest that deletion of *Tgfb2* improves cell survival of a small group of the hearts with *Dicer1* inactivated.

4. Discussion

miRNAs have recently emerged as highly attractive therapeutic targets/reagents for various cardiovascular diseases.^{23–25} As such, it has become imperative to better understand the function of miRNAs during cardiovascular system development. Previous studies have tested the cardiogenic roles of global miRNA biosynthesis through heart-specific deletion of *Dicer1* using different Cre drivers. Deletion of *Dicer1* in cardiac progenitor cells using an *Nkx2.5-Cre* driver led to delayed ventricular development, pericardial oedema, and embryonic death at E12.5.²⁷ Deletion of *Dicer1* using an independent *Nkx2.5-Cre*

driver, which inactivates targets with subtly different spatiotemporal kinetics, led to abnormal outflow-tract patterning.²⁸ Myocardial inactivation of *Dicer1* at late gestation using *MHC-Cre* resulted in dilated cardiomyopathy, heart failure, and early postnatal lethality.²⁹ These results collectively indicate that miRNAs play complex roles at different cardiogenic stages. To reveal the effect of blocking miRNA biosynthesis at midgestation, a stage that has not been evaluated in previous studies, we specifically inactivated *Dicer1* using *cTnt-Cre*, which efficiently inactivates target genes in cardiomyocytes at E10.5–11.5.^{30,37} Our current study provides novel insights into the cardiogenic roles of the miRNA regulatory machinery.

A major conclusion of this study is that elevated TGF β signalling plays an important role in the heart defects caused by *Dicer1* inactivation. We reveal that TGF β signalling is negatively regulated by the miRNA machinery during cardiogenesis. Ectopic expression of constitutively active TGFBR1 arrested heart development at the primitive tube stage at E9.5, suggesting that hearts are sensitive to uncontrolled TGF β activity at the looping stage.¹⁵ How increased TGF β activity affects heart development after chamber formation has not been reported. We show that exogenous TGF β 1 significantly increases cell death, and that pharmacological blockade of TGF β activity alleviates the cell death abnormality caused by myocardial inactivation of *Dicer1*. To reveal the *in vivo* relevance of enhanced TGF β activity in *Dicer1* mutant hearts, we applied a genetic approach to reduce TGF β activity by deletion of *Tgfr2* in mice with *Dicer1* myocardial inactivation. *Tgfr2* encodes the only known Type II receptor of TGFBR1. Significantly, a small portion of double-mutant embryos survived beyond E16.5, the stage at which no *Dicer1*-sKO mutant could survive to. Our results support the notion that normal TGF β activity is essential for heart development after chamber formation, and that uncontrolled TGF β activity is a major contributing factor for the heart defects in *Dicer1*-inactivated embryos.

We previously reported that myocardial inactivation of *Tgfr2* led to a minor heart defect with a low penetrance (10%).¹³ However, we did not observe any heart defect in *Tgfr2* sKO embryos in this study. This discrepancy is likely caused by different mouse backgrounds used in the two studies. In the previous study, C57BL/6 mice were used, while in the current study the mice are on a mixed C57BL/6 \times 129s6 background.

Reducing TGF β activity only partially alleviated the cardiac defects caused by *Dicer1* inactivation. This result is expected, as other cardiogenic signalling pathways are likely also disrupted in *Dicer1*-inactivated hearts. The cardiac phenotypes of *Dicer1*-inactivated embryos are most likely caused by the combined effects of abnormal expression of multiple genes (see Supplementary material online, Table S1). Interaction between endocardial and myocardial cells is important for normal myocardial wall development. For example, the endocardium can promote trabeculation of the myocardium through EGF signalling.^{44,45} It is possible that increased TGF β activity in the myocardium can lead to abnormal development of endocardial cells, which in turn contributes to the abnormalities in the mutant myocardial wall.

We provide evidence that the 3' UTR of *Tgfr1* is directly targeted by miR98, miR128, and miR142. miR98 belongs to the let7 miRNA family, in which all members share identical seed sequences. Therefore, *Tgfr1* is likely also targeted by other let7 members. The function of let7/miR98 has been heavily studied in stem cell differentiation/proliferation, tumour suppression, and neural development.⁴⁶ Studies of miR128 and miR142 have mainly focused on their role in cancer biology.^{47,48} We provide the first evidence that these three miRNAs regulate cardiomyogenesis through directly repressing TGFBR1 expression.

Considering the broad roles of TGF β signalling in numerous biological/pathological processes, we speculate that these miRNAs also regulate TGF β activity in other cell types.

Spongy myocardial wall due to non-compaction is a novel phenotype observed in the current study that has not been reported in other *Dicer1* inactivation models. Non-compaction in human patients can cause congestive heart failure, arrhythmias, thromboembolic complications, and sudden death.^{49–51} Mouse models with non-compaction have been increasingly reported and include *Fkbp12*,⁵² *Smad7*,⁵³ *Crc*,⁵⁴ *Vangl2*,⁵⁵ *Daam1*,⁵⁶ and *Mib1*⁵⁷ knockout mice and *Bmp10*⁵⁸ overexpression mice. We demonstrated for the first time that miRNA biosynthesis is required for normal myocardial wall compaction. It is noteworthy that *Fkbp12*^{59,60} and *Smad7*⁶¹ negatively regulate TGF β activities. Therefore, increased TGF β activity is the common feature of three non-compaction mouse models, which include *Fkbp12*^{-/-},⁵² *Smad7* ^{Δ MH2-/-},⁵³ and *cTnt-Cre;Dicer1*^{loxP/loxP} mice, and may thus play an aetiological role in non-compaction. This hypothesis is supported by our discovery that surviving *Tgfr2;Dicer1* double-mutant embryos did not show the spongy wall defect.

In summary, our study on myocardial inactivation of *Dicer1* during midgestation reveals critical roles of miRNA biosynthesis for myocardial wall morphogenesis. Our data support the idea that miRNA-mediated repression of *Tgfr1* expression prevents excess TGF β signalling in cardiomyocytes, thereby supporting normal heart development.

Supplementary material

Supplementary material is available at *Cardiovascular Research* online.

Acknowledgements

We thank Drs E. Olson (UT SouthWestern), H. Moses (VUMC), S. Kubalak (University of South Carolina), W. Shou (Indiana University), and M. Merkenschlager (MRC Clinical Sciences Centre) for providing necessary reagents. We thank Dr Y.S. Yoon (Emory University) for suggestions on using the molecular beacon. We thank UAB Heflin Genetics Core for performing microarray analysis and the UAB Flow Cytometry Facility core for sorting cardiomyocytes.

Conflict of interest: none declared.

Funding

This project is supported by a grant-in-aid (12GRNT11650007) from American Heart Association awarded to K.J.

References

- Doetschman T, Barnett JV, Runyan RB, Camenisch TD, Heimark RL, Granzier HL, Conway SJ, Azhar M. Transforming growth factor beta signaling in adult cardiovascular diseases and repair. *Cell Tissue Res* 2012;**347**:203–223.
- Judge DP, Rouf R, Habashi J, Dietz HC. Mitral valve disease in Marfan syndrome and related disorders. *J Cardiovasc Transl Res* 2011;**4**:741–747.
- Conway SJ, Doetschman T, Azhar M. The inter-relationship of Periostin, TGFbeta, and BMP in heart valve development and valvular heart diseases. *Scientific World Journal* 2011;**11**:1509–1524.
- Arthur HM, Bamforth SD. TGFbeta signaling and congenital heart disease: insights from mouse studies. *Birth Defects Res A Clin Mol Teratol* 2011;**91**:423–434.
- DeLaughter DM, Saint-Jean L, Baldwin HS, Barnett JV. What chick and mouse models have taught us about the role of the endocardium in congenital heart disease. *Birth Defects Res A Clin Mol Teratol* 2011;**91**:511–525.
- Shi Y, Massague J. Mechanisms of TGF-beta signaling from cell membrane to the nucleus. *Cell* 2003;**113**:685–700.
- Ten Dijke P, Hill CS. New insights into TGF-beta-Smad signalling. *Trends Biochem Sci* 2004;**29**:265–273.

8. Lee MK, Pardoux C, Hall MC, Lee PS, Warburton D, Qing J, Smith SM, Derynck R. TGF-beta activates Erk MAP kinase signalling through direct phosphorylation of ShcA. *EMBO J* 2007;**26**:3957–3967.
9. Tran-Fadulu V, Pannu H, Kim DH, Vick GW III, Lonsford CM, Lafont AL, Boccalandro C, Smart S, Peterson KL, Hain JZ, Willing MC, Coselli JS, LeMaire SA, Ahn C, Byers PH, Milewicz DM. Analysis of multigenerational families with thoracic aortic aneurysms and dissections due to TGFBR1 or TGFBR2 mutations. *J Med Genet* 2009;**46**:607–613.
10. Sorrentino A, Thakur N, Grimbsy S, Marcusson A, von Bulow V, Schuster N, Zhang S, Heldin CH, Landstrom M. The type I TGF-beta receptor engages TRAF6 to activate TAK1 in a receptor kinase-independent manner. *Nat Cell Biol* 2008;**10**:1199–1207.
11. Sanford LP, Ormsby I, Gittenberger-de Groot AC, Sariola H, Friedman R, Boivin GP, Cardell EL, Doetschman T. TGFbeta2 knockout mice have multiple developmental defects that are non-overlapping with other TGFbeta knockout phenotypes. *Development* 1997;**124**:2659–2670.
12. Bartram U, Molin DG, Wisse LJ, Mohamad A, Sanford LP, Doetschman T, Speer CP, Poelmann RE, Gittenberger-de Groot AC. Double-outlet right ventricle and overriding tricuspid valve reflect disturbances of looping, myocardialization, endocardial cushion differentiation, and apoptosis in TGF-beta(2)-knockout mice. *Circulation* 2001;**103**:2745–2752.
13. Jiao K, Langworthy M, Batts L, Brown CB, Moses HL, Baldwin HS. Tgfbeta signaling is required for atrioventricular cushion mesenchyme remodeling during in vivo cardiac development. *Development* 2006;**133**:4585–4593.
14. Sridurongrit S, Larsson J, Schwartz R, Ruiz-Lozano P, Kaartinen V. Signaling via the Tgf-beta type I receptor Alk5 in heart development. *Dev Biol* 2008;**322**:208–218.
15. Chang MJ, Frenkel PA, Lin Q, Yamada M, Schwartz RJ, Olson EN, Overbeek P, Schneider MD, Yumada M. A constitutive mutation of ALK5 disrupts cardiac looping and morphogenesis in mice. *Dev Biol* 1998;**199**:72–79.
16. Dean JC. Marfan syndrome: clinical diagnosis and management. *Eur J Hum Genet* 2007;**15**:724–733.
17. Mizuguchi T, Matsumoto N. Recent progress in genetics of Marfan syndrome and Marfan-associated disorders. *J Hum Genet* 2007;**52**:1–12.
18. Akutsu K, Morisaki H, Takeshita S, Sakamoto S, Tamori Y, Yoshimuta T, Yokoyama N, Nonogi H, Ogino H, Morisaki T. Phenotypic heterogeneity of Marfan-like connective tissue disorders associated with mutations in the transforming growth factor-beta receptor genes. *Circ J* 2007;**71**:1305–1309.
19. Loeys BL, Chen J, Neptune ER, Judge DP, Podowski M, Holm T, Meyers J, Leitch CC, Katsanis N, Sharifi N, Xu FL, Myers LA, Spevak PJ, Cameron DE, De Backer J, Hellemans J, Chen Y, Davis EC, Webb CL, Kress W, Coucke P, Rifkin DB, De Paepe AM, Dietz HC. A syndrome of altered cardiovascular, craniofacial, neurocognitive and skeletal development caused by mutations in TGFBR1 or TGFBR2. *Nat Genet* 2005;**37**:275–281.
20. van de Laar IM, Oldenburg RA, Pals G, Roos-Hesselink JW, de Graaf BM, Verhagen JM, Hoedemaekers YM, Willemsen R, Severijnen LA, Venselaar H, Vriend G, Pattynama PM, Collee M, Majoor-Krakauer D, Poldermans D, Frohn-Mulder IM, Micha D, Timmermans J, Hilhorst-Hofstee Y, Bierma-Zeinstra SM, Willems PJ, Kros JM, Oei EH, Oostra BA, Wessels MW, Bertoli-Avella AM. Mutations in SMAD3 cause a syndromic form of aortic aneurysms and dissections with early-onset osteoarthritis. *Nat Genet* 2011;**43**:121–126.
21. Lindsay ME, Schepers D, Bolar NA, Doyle JJ, Gallo E, Fert-Bober J, Kempers MJ, Fishman EK, Chen Y, Myers L, Bjeda D, Oswald G, Elias AF, Levy HP, Anderlid BM, Yang MH, Bongers EM, Timmermans J, Braverman AC, Canham N, Mortier GR, Brunner HG, Byers PH, Van Eyk J, Van Laer L, Dietz HC, Loeys BL. Loss-of-function mutations in TGFBR2 cause a syndromic presentation of thoracic aortic aneurysm. *Nat Genet* 2012;**44**:922–927.
22. Boileau C, Guo DC, Hanna N, Regalado ES, Detaint D, Gong L, Varret M, Prakash SK, Li AH, d'Indy H, Braverman AC, Grandchamp B, Kwartler CS, Gouya L, Santos-Cortez RL, Abifadel M, Leal SM, Muti C, Shendure J, Gross MS, Rieder MJ, Vahanian A, Nickerson DA, Michel JB, National Heart Lung and Blood Institute Go Exome Sequencing Project, Jordeau G, Milewicz DM. TGFBR2 mutations cause familial thoracic aortic aneurysms and dissections associated with mild systemic features of Marfan syndrome. *Nat Genet* 2012;**44**:916–921.
23. Cordes KR, Srivastava D. MicroRNA regulation of cardiovascular development. *Circ Res* 2009;**104**:724–732.
24. Malizia AP, Wang DZ. MicroRNAs in cardiomyocyte development. *Wiley Interdiscip Rev Syst Biol Med* 2011;**3**:183–190.
25. Chen J, Wang DZ. microRNAs in cardiovascular development. *J Mol Cell Cardiol* 2012;**52**:949–957.
26. Bartel DP. MicroRNAs: target recognition and regulatory functions. *Cell* 2009;**136**:215–233.
27. Zhao Y, Ransom JF, Li A, Vedantham V, von Drehle M, Muth AN, Tsuchihashi T, McManus MT, Schwartz RJ, Srivastava D. Dysregulation of cardiogenesis, cardiac conduction, and cell cycle in mice lacking miRNA-1-2. *Cell* 2007;**129**:303–317.
28. Saxena A, Tabin CJ. miRNA-processing enzyme Dicer is necessary for cardiac outflow tract alignment and chamber septation. *Proc Natl Acad Sci USA* 2010;**107**:87–91.
29. Chen JF, Murchison EP, Tang R, Callis TE, Tatsuguchi M, Deng Z, Rojas M, Hammond SM, Schneider MD, Selzman CH, Meissner G, Patterson C, Hannon GJ, Wang DZ. Targeted deletion of Dicer in the heart leads to dilated cardiomyopathy and heart failure. *Proc Natl Acad Sci USA* 2008;**105**:2111–2116.
30. Jiao K, Kulesha H, Tompkins K, Zhou Y, Batts L, Baldwin HS, Hogan BL. An essential role of Bmp4 in the atrioventricular septation of the mouse heart. *Genes Dev* 2003;**17**:2362–2367.
31. Cobb BS, Nesterova TB, Thompson E, Hertweck A, O'Connor E, Godwin J, Wilson CB, Brockdorff N, Fisher AG, Smale ST, Merckenschlager M. T cell lineage choice and differentiation in the absence of the RNase III enzyme Dicer. *J Exp Med* 2005;**201**:1367–1373.
32. Chytil A, Magnuson MA, Wright CV, Moses HL. Conditional inactivation of the TGF-beta type II receptor using Cre:Lox. *Genesis* 2002;**32**:73–75.
33. Jiao K, Zhou Y, Hogan BL. Identification of mZnfb, a mouse Kruppel-like transcriptional repressor, as a novel nuclear interaction partner of Smad1. *Mol Cell Biol* 2002;**22**:7633–7644.
34. Rybkin II, Markham DW, Yan Z, Bassel-Duby R, Williams RS, Olson EN. Conditional expression of SV40 T-antigen in mouse cardiomyocytes facilitates an inducible switch from proliferation to differentiation. *J Biol Chem* 2003;**278**:15927–15934.
35. Ban K, Wile B, Kim S, Park HJ, Byun J, Cho KW, Saafir T, Song MK, Yu SP, Wagner M, Bao G, Yoon YS. Purification of cardiomyocytes from differentiating pluripotent stem cells using molecular beacons that target cardiomyocyte-specific mRNA. *Circulation* 2013;**128**:1897–1909.
36. Song L, Fassler R, Mishina Y, Jiao K, Baldwin HS. Essential functions of Alk3 during AV cushion morphogenesis in mouse embryonic hearts. *Dev Biol* 2007;**301**:276–286.
37. Chen JW, Zhou B, Yu QC, Shin SJ, Jiao K, Schneider MD, Baldwin HS, Bergelson JM. Cardiomyocyte-specific deletion of the coxsackievirus and adenovirus receptor results in hyperplasia of the embryonic left ventricle and abnormalities of sinuatrial valves. *Circ Res* 2006;**98**:923–930.
38. Zeller R, Bloch KD, Williams BS, Arceci RJ, Seidman CE. Localized expression of the atrial natriuretic factor gene during cardiac embryogenesis. *Genes Dev* 1987;**1**:693–698.
39. Nakao A, Afrakhte M, Moren A, Nakayama T, Christian JL, Heuchel R, Itoh S, Kawabata M, Heldin NE, Heldin CH, ten Dijke P. Identification of Smad7, a TGFbeta-inducible antagonist of TGF-beta signalling. *Nature* 1997;**389**:631–635.
40. Nagarajan RP, Zhang J, Li W, Chen Y. Regulation of Smad7 promoter by direct association with Smad3 and Smad4. *J Biol Chem* 1999;**274**:33412–33418.
41. Piek E, Moustakas A, Kurisaki A, Heldin CH, ten Dijke P. TGF-(beta) type I receptor/ALK-5 and Smad proteins mediate epithelial to mesenchymal transdifferentiation in NMuMG breast epithelial cells. *J Cell Sci* 1999;**112**(Pt 24):4557–4568.
42. DaCosta Byfield S, Major C, Laping NJ, Roberts AB. SB-505124 is a selective inhibitor of transforming growth factor-beta type I receptors ALK4, ALK5, and ALK7. *Mol Pharmacol* 2004;**65**:744–752.
43. Carvalho RL, Itoh F, Goumans MJ, Lebrin F, Kato M, Takahashi S, Ema M, Itoh S, van Rooijen M, Bertolino P, Ten Dijke P, Mummery CL. Compensatory signalling induced in the yolk sac vasculature by deletion of TGFbeta receptors in mice. *J Cell Sci* 2007;**120**:4269–4277.
44. Gassmann M, Casagrande F, Orioli D, Simon H, Lai C, Klein R, Lemke G. Aberrant neural and cardiac development in mice lacking the ErbB4 neuregulin receptor. *Nature* 1995;**378**:390–394.
45. Lee KF, Simon H, Chen H, Bates B, Hung MC, Hauser C. Requirement for neuregulin receptor erbB2 in neural and cardiac development. *Nature* 1995;**378**:394–398.
46. Mondol V, Pasquinelli AE. Let's make it happen: the role of let-7 microRNA in development. *Curr Top Dev Biol* 2012;**99**:1–30.
47. Nanta R, Kumar D, Meeker D, Rodova M, Van Veldhuizen PJ, Shankar S, Srivastava RK. NVP-LDE-225 (Erismodegib) inhibits epithelial-mesenchymal transition and human prostate cancer stem cell growth in NOD/SCID IL2Rgamma null mice by regulating Bmi-1 and microRNA-128. *Oncogenesis* 2013;**2**:e42.
48. Kwahian W, Lenze D, Alles J, Motsch N, Barth S, Doll C, Imig J, Hummel M, Tinguely M, Trivedi P, Lulitanond V, Meister G, Renner C, Grasser FA. MicroRNA-142 is mutated in about 20% of diffuse large B-cell lymphoma. *Cancer Med* 2012;**1**:141–155.
49. Weisz SH, Limongelli G, Pacileo G, Calabro P, Russo MG, Calabro R, Vatta M. Left ventricular non compaction in children. *Congenit Heart Dis* 2010;**5**:384–397.
50. Finsterer J. Left ventricular non-compaction and its cardiac and neurologic implications. *Heart Fail Rev* 2010;**15**:589–603.
51. Chen H, Zhang W, Li D, Cordes TM, Mark Payne R, Shou W. Analysis of ventricular hypertrabeculation and noncompaction using genetically engineered mouse models. *Pediatr Cardiol* 2009;**30**:626–634.
52. Shou W, Aghdasi B, Armstrong DL, Guo Q, Bao S, Chang MJ, Mathews LM, Schneider MD, Hamilton SL, Matzuk MM. Cardiac defects and altered ryanodine receptor function in mice lacking FKBP12. *Nature* 1998;**391**:489–492.
53. Chen Q, Chen H, Zheng D, Kuang C, Fang H, Zou B, Zhu W, Bu G, Jin T, Wang Z, Zhang X, Chen J, Field LJ, Rubart M, Shou W, Chen Y. Smad7 is required for the development and function of the heart. *J Biol Chem* 2009;**284**:292–300.
54. Phillips HM, Rhee HJ, Murdoch JN, Hildreth V, Peat JD, Anderson RH, Copp AJ, Chaudhry B, Henderson DJ. Disruption of planar cell polarity signaling results in congenital heart defects and cardiomyopathy attributable to early cardiomyocyte disorganization. *Circ Res* 2007;**101**:137–145.
55. Phillips HM, Hildreth V, Peat JD, Murdoch JN, Kobayashi K, Chaudhry B, Henderson DJ. Non-cell-autonomous roles for the planar cell polarity gene Vangl2 in development of the coronary circulation. *Circ Res* 2008;**102**:615–623.
56. Li D, Hallett MA, Zhu W, Rubart M, Liu Y, Yang Z, Chen H, Haneline LS, Chan RJ, Schwartz RJ, Field LJ, Atkinson SJ, Shou W. Dishevelled-associated activator of

- morphogenesis 1 (Daam1) is required for heart morphogenesis. *Development* 2011;**138**: 303–315.
57. Luxan G, Casanova JC, Martinez-Poveda B, Prados B, D'Amato G, MacGrogan D, Gonzalez-Rajal A, Dobarro D, Torroja C, Martinez F, Izquierdo-Garcia JL, Fernandez-Friera L, Sabater-Molina M, Kong YY, Pizarro G, Ibanez B, Medrano C, Garcia-Pavia P, Gimeno JR, Monserrat L, Jimenez-Borreguero LJ, de la Pompa JL. Mutations in the NOTCH pathway regulator MIB1 cause left ventricular noncompaction cardiomyopathy. *Nat Med* 2013;**19**:193–201.
58. Pashmforoush M, Lu JT, Chen H, Amand TS, Kondo R, Pradervand S, Evans SM, Clark B, Feramisco JR, Giles W, Ho SY, Benson DW, Silberbach M, Shou W, Chien KR. Nkx2–5 pathways and congenital heart disease; loss of ventricular myocyte lineage specification leads to progressive cardiomyopathy and complete heart block. *Cell* 2004;**117**:373–386.
59. Wang T, Li BY, Danielson PD, Shah PC, Rockwell S, Lechleider RJ, Martin J, Manganaro T, Donahoe PK. The immunophilin FKBP12 functions as a common inhibitor of the TGF beta family type I receptors. *Cell* 1996;**86**:435–444.
60. Wang T, Donahoe PK. The immunophilin FKBP12: a molecular guardian of the TGF-beta family type I receptors. *Front Biosci* 2004;**9**:619–631.
61. Briones-Orta MA, Tecalco-Cruz AC, Sosa-Garrocho M, Caligaris C, Macias-Silva M. Inhibitory Smad7: emerging roles in health and disease. *Curr Mol Pharmacol* 2011;**4**: 141–153.